J. Nano- Electron. Phys.
3 (2011) No1, P. 639-646

PACS number: 61.46.Df

PHOTOLUMINESCENCE AND EPR STUDIES OF ZnS NANOPARTICLES Co-DOPED WITH Mn AND Te

***A. Divya*[1], *B.K. Reddy*[1], *S. Sambasivam*[2], *P. Sreedhara Reddy*[1]**

[1] Department of Physics,
S.V. University, Tirupati-517502, A.P., India
E-mail: divyaphy07@gmail.com

[2] Department of Physics,
Pukyong National University, Busan, South Korea

ZnS nanoparticles Co-doped with Mn and Te ($x = 0.05$ and 0.10) have been synthesized for the first time by chemical co-precipitation method, thiophenol is used to passivate the surface of the particles. The as-prepared samples were amorphous in nature. Nanocrystallinity was induced after calcining the samples at 300°C/2hrs. The obtained nanoparticles were subjected to X-ray diffraction (XRD), Energy Dispersive Analysis of X-rays (EDAX), Transmission Electron Microscopy (TEM), Photoluminescence (PL) and Electron Paramagnetic Resonance (EPR) studies. All the samples exhibited cubic structure and the particle size was found to be 3-5 nm. EDAX revealed that the compositions did not deviate much from the target compositions. The photoluminescence studies showed emission in the red region and the emission wavelength is varied with composition. The Electron Paramagnetic Resonance (EPR) spectra showed paramagnetic nature of the samples at room temperature. EPR and PL results were quite consistent with each other.

Keywords: *NANOPARTICLES, ZnS, TRANSMISSION ELECTRON MICROSCOPY (TEM), PHOTOLUMINESCENCE (PL), ELECTRON PARAMAGNETIC RESONANCE (EPR).*

(Received 04 February 2011)

1. INTRODUCTION

In recent years, low dimensional structures and nanometer-sized semiconductor particles have received much attention due to their novel unique properties and potential applications in optoelectronic industry [1, 2]. The structure, electronic, optical and magnetic properties of nanoparticles differ from those of their corresponding bulk form due to quantum confinement effects [3, 4]. All these properties are various manifestations of the so-called quantum size effect which arises due to the increasing quantum confinement of the electrons and holes with diminishing size of the crystallites and the consequent changes in the electronic structures. However, when the dimensions of the crystallites becomes comparable or less than the Bohr radius of the exciton wave function, there is a significant change in the properties. In molecular terminology, this corresponds to the widening of the energy gap between the highest occupied molecular orbital (HOMO) and lowest unoccupied molecular orbital (LUMO) as the size decreases. The ability to tune the band gap of semiconductor to suit any specific application by tailoring the size of the particles has many exciting technological implications.

As a nontoxic II-VI semiconductor material, ZnS is chemically more stable and technologically better than other semiconductor materials (such as ZnSe), so it is considered to be a promising host material. Both transition metal ions (e.g. Mn^{2+} [5,6], Cu^{2+} [7]) and rare earth ions (e.g. Eu^{3+} [8,9]) have been incorporated into ZnS nanostructures by various physical and chemical methods. These doped ZnS semiconductor materials have a wide range of applications in electroluminescence devices, phosphors, light emitting displays, optical sensors, etc. Among these nanostructured materials, zinc sulfide nanoparticles doped with Mn^{2+} ions (ZnS:Mn) are of special interest due to the highly effective luminescence [10]. In addition, the introduction of magnetic Mn^{2+} ions into nonmagnetic ZnS semiconductor nanoparticles allows for the generation of diluted magnetic semiconductor (DMS), which can exhibit interesting magnetic and magneto-optical properties. The recombination of magnetic spin and electron charge in such magnetic nanostructures may also provide unparalleled opportunities for the rapidly emerging field of spintronics [11]. Electron Paramagnetic Resonance (EPR) technique has been widely used to obtain an insight about the local crystal field effects and symmetry around Mn^{2+} ions in ZnS lattice [12]. In this study, the photoluminescence (PL) and electron paramagnetic resonance (EPR) properties of ZnS nanoparticles co-doped with Mn and Te synthesized by using chemical co-precipitation method are reported for the first time.

2. EXPERIMENTAL

Zinc acetate, manganese acetate, sodium sulfide and tellurium dioxide (Sigma Aldrich, Germany) were used as starting compounds. Appropriate amounts of these were weighed according to the stoichiometry to obtain target compositions of Mn and Te ($x = 0.05$ and 0.10). The source materials were dissolved in 100 ml methanol to make 0.1 *M* solutions. The stoichiometric solution was taken in a burette and was added drop wise to a mixture of Na_2S (0.1 M) + 50 ml H_2O + 2 ml of thiophenol + 100 ml of methanol with continuous stirring until a fine precipitate was obtained. The precipitated solution was kept under constant stirring for 20 hrs. The precipitate was filtered out and was washed thoroughly with de-ionized water. The as-prepared samples (the precipitates) were amorphous in nature as revealed by XRD studies. Calcining the samples at 300°C/2hrs. induced nano-crystallinity. EDAX technique was employed for the compositional analysis of the samples. XRD studies were carried out using Seifert 3003TT X-ray diffractometer. Grain size studies were done using TECHNAI-TEM FEI Transmission Electron Microscope (TEM), operated at an accelerating voltage of 100-200 KV. Samples for TEM studies were prepared by dispersing the powders in methanol. Photoluminescence spectra were recorded at room temperature in the wavelength range of 400-700 nm using PTI (Photon Technology International) Fluorimeter with a Xe-arc lamp of power 60 *W*. An excitation wavelength (λ_{exc}) of 320 nm was used. Electron Paramagnetic Resonance (EPR) Spectra for powder samples were recorded at room temperature using X-band Bruker ER-041 Spectrometer in the frequency range of 8.8-9.6 GHz.

3. RESULTS AND DISCUSSION

3.1 Chemical and Structural Analysis

In order to confirm the presence of Mn and Te ions in the material, we perform the EDAX study of co-doped samples. The typical EDAX spectrum of ZnS nanoparticles co-doped with Mn and Te (x = 0.05) is shown in Fig. 1.

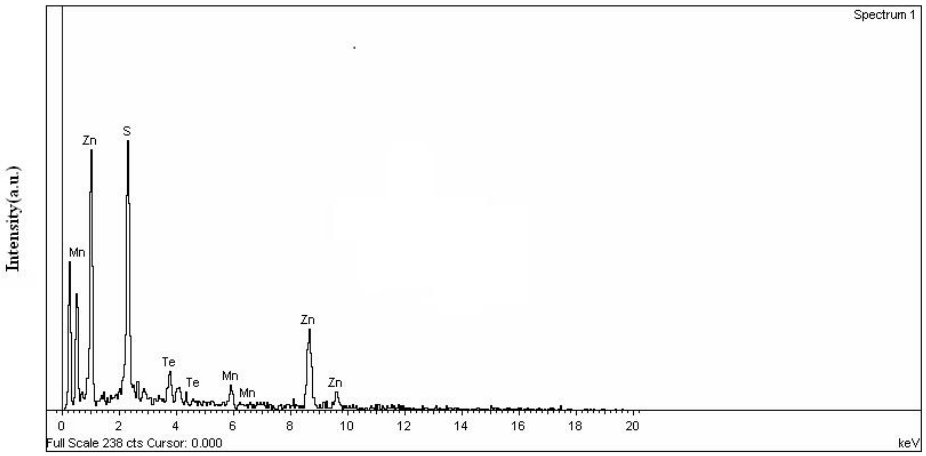

Fig. 1 *– EDAX spectrum of ZnS nanoparticles co-doped with Mn and Te (x = 0.05)*

It is clear that chemical compositions of the constituents in the samples, obtained from EDAX did not deviate much from the starting material composition. Crystallinity, size and phase of the nanoparticles were characterized by XRD as shown in Fig. 2.

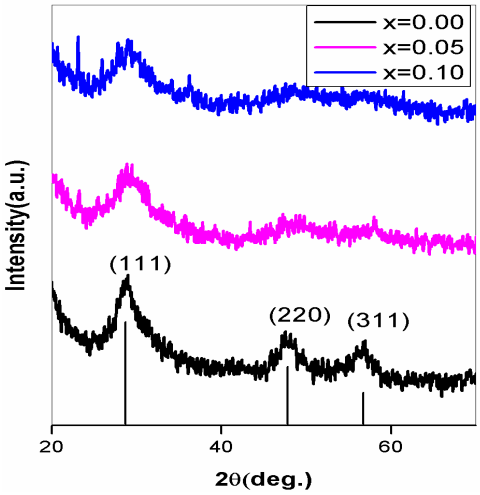

Fig. 2 *– XRD patterns of ZnS nanoparticles co-doped with Mn and Te (x = 0, 0.05 and 0.10). The peak positions are marked for the cubic ZnS (JCPDS No.80-0020).*

Peak positions indicate the formation of zincblende crystal structure with three most preferred orientations [111], [220] and [311]. No other impurity peaks were observed indicating the formation of pure cubic phase of ZnS only, the broadening of the diffraction peaks shows the formation of nano sized particles. The average nano crystallite sizes are calculated from fullwidth at half maximum (β) of XRD peaks using Debye-Scherrer's formula [13].

$$D = 0.94\lambda/\beta\cos\theta \quad (1)$$

Where D is the average particle size, β is the full width at half maximum (FWHM) of XRD peak expressed in radians and θ is the position of the diffraction peak. From the calculations, the average diameter of the particles lies in the range of 3-5 nm. Typical TEM image of ZnS nanoparticles co-doped with Mn and Te (x = 0.05) is shown in Fig. 3.

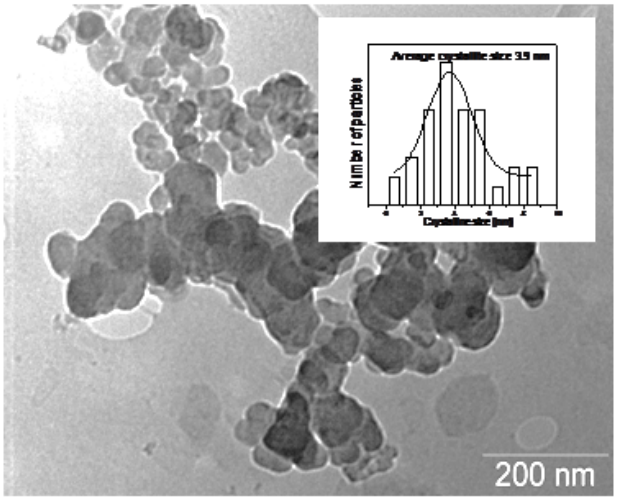

Fig. 3 *– Typical TEM micrograph of ZnS nanoparticles co-doped with Mn and Te (*x = 0.05*), with inset showing the size distribution plot.*

The crystallites in the sample with x = 0.05 are found to be isolated and spherical in shape. The distribution plot fitted to a Gaussian profile is shown as inset in Fig. 3. This shows that the size of most of the particles lies in a narrow range of 3-6 nm. The average particle size obtained from TEM is 3.9 nm for the samples of this composition, which is comparable with that of the crystallite size estimated from XRD measurements.

3.2. PHOTOLUMINESCENCE STUDIES

Fig. 4 shows the PL emission spectra recorded at room temperature, with an excitation wavelength of 320 nm, for the present ZnS nanoparticles co-doped with Mn and Te (x = 0.05 and 0.10).

It is obvious that the emission is peaked at 605 nm and 609 nm for x = 0.05 and 0.10 samples respectively. The emission wavelength is red shifted with increasing dopant (Mn and Te) content and also luminescence intensity

decreases gradually. The luminescence intensity is maximum for $x = 0.05$ samples and it quenches for $x = 0.10$ samples. Similar luminescence intensity drop was also observed by Rao et al. [14] in $(ZnS)_{1-x}$ $(MnTe)_x$ bulk powders prepared by solid state reaction method. Son et al. [15] reported an emission wavelength of about 580 nm in 5 % Mn doped ZnS nanoparticles having an average grain size of 7.3 nm. They also observed appreciable drop in emission intensity with increasing Mn content (5-10 at.%).

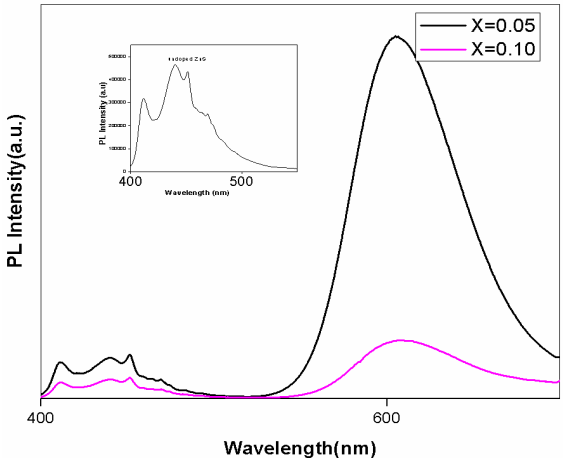

Fig. 4 *– PL spectra ($\lambda_{exc} = 320$ nm) of ZnS nanoparticles co-doped with Mn and Te ($x = 0.05$ and 0.10), undoped ZnS PL spectrum shown in inset*

The inset in Fig. 4 shows PL spectrum for undoped ZnS nanoparticles recorded in the present work for comparison. Blue emission peaking at 440 nm with two less prominent sub bands at 411 nm and 451 nm are observed for undoped ZnS nanoparticles. Other workers [16, 19] have also reported similar blue emission in undoped ZnS nanoparticles. In the present investigation, undoped ZnS nanoparticles showed blue emission and yellow emission was observed in Mn doped ZnS nanoparticles, which was not shown here. Whereas Mn and Te co-doped ZnS nanoparticles exhibited intense red emission. The red shift in the emission wavelength observed in the present study is a good example of energy transfer process, wherein Mn ions transfer energy to Te ions and the red emission occurs from Te ions through $^3T_1 \rightarrow {}^1A_1$ [20] transition. In the present nanoparticles of ZnS: (Mn, Te) the red emission may be due to Mn^{2+} surrounded by a mixture of S and Te ions or even by Te ions only [21]. Rao et al. [14] have earlier reported composition independent broad emission bands in the red region centered around 650 nm in $(ZnS)_{1-x}$ $(MnTe)_x$ bulk powders for x in the range 0.02-0.25. Benalloul et al. [21] observed emissions peaking at 600 nm in $Zn_{1-x}Mn_xS_{1-y}Te|_y$ thin films with $x = 0.04$ and $y = 0.06$ at low temperatures. No reports on PL spectra of ZnS nanoparticles co-doped with Mn and Te are available in literature for comparison.

3.3. ELECTRON PARAMAGNETIC RESONANCE STUDIES

EPR study is one of the best tools because of its high absolute sensitivity and the ability to detect small changes in the local crystal field, resulting

from different localization of the paramagnetic impurity ions. Also it is used to study the changes in the configuration and nature of the neighboring ligands [22]. Fig. 5 shows the EPR spectra of the present samples recorded at room temperature (300 K) in the frequency range of 8.8-9.6 GHz. When the magnetic field is applied to the sample, the energy levels of Mn^{2+} (^{55}Mn, $I = 5/2$) split due to Zeeman interaction. In addition, the interaction of the electronic spin with the nuclear spin gives rise to the hyperfine interaction.

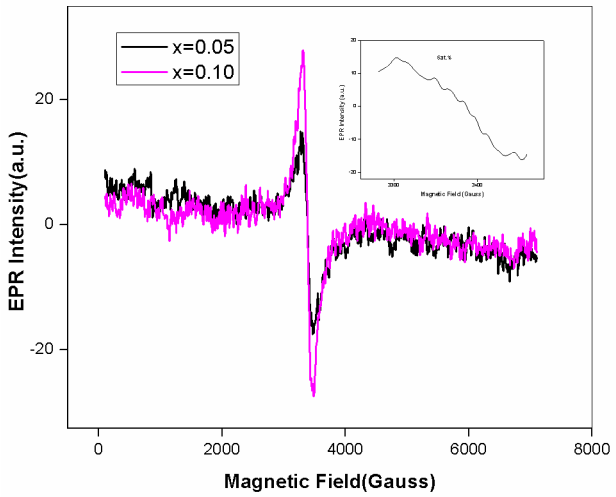

Fig. 5 *– EPR spectra of ZnS nanoparticles co-doped with Mn and Te (*$x = 0.05$ *and* 0.10*) at room temperature, inset shows six-line hyperfine structure pattern for (*$x = 0.05$*) samples*

The EPR spectra of the Mn^{2+} centers in nanocrystalline cubic ZnS: Mn are described by the following Spin Hamiltonian, with usual notation [23].

$$H = g\mu_B \vec{S}.\vec{B} + A\vec{S}.\vec{I} + \frac{a}{6}\left[(S_x^4 + S_y^4 + S_z^4) + \frac{1}{5}S(S+1)(3S^2 + 3S - 1)\right] + D\left[S_z^2 - \frac{1}{3}S(S+1)\right] + \mu_N g_N \vec{B}.\vec{I}. \quad (1)$$

The first two terms on the right hand side represent the main interactions of the $S = 5/2$ electron spin with the external magnetic field B (the electron Zeeman interaction) and the hyperfine interaction with the $I = 5/2$ nuclear spin of the ^{55}Mn (100 % abundance) isotope, respectively. The next two terms describe the interaction of the electron spin with the local crystal field, characterized by the Zero-Field Splitting (ZFS) cubic a and axial D parameters, and the last term corresponds to the nuclear Zeeman interaction of the $I = 5/2$ nuclear spin with the external magnetic field B.

From the figure it is obvious that for low dopant Mn and Te ($x = 0.05$) concentration six-line hyperfine structure appears in the central region of the spectrum shown in the inset. This sextet pattern is characteristic of

Mn^{2+} ions with a nuclear spin $I = 5/2$. Further, with increasing dopant (Mn and Te $x = 0.10$) concentration, the characteristic six-line pattern disappears and a broad signal appears. This broad line could be due to clustered manganese ions, which strongly influence one another through their magnetic moments. We obtained the g value (2.0046) using Rubbins and Beanny relation [24] for the present ZnS: Mn, Te samples and confirms the paramagnetic nature at room temperature. Rao et al. [25] also observed similar disappearance of hyperfine structure for higher concentrations of Mn^{2+} in $(ZnS)_{1-x}(MnTe)_x$ powder samples and also reported similar g-value (~ 2.003).

Our EPR and PL results are in good agreement with each other. The red emission of the present samples is maximum for $x = 0.05$ concentration, and subsequently, it quenched with increasing Mn and Te ($x = 0.10$) content. Whereas in EPR, $x = 0.05$ samples exhibited six-line hyperfine structure pattern and this pattern disappears for $x = 0.10$ samples.

4.CONCLUSIONS

We have successfully prepared ZnS nanoparticles co-doped with Mn and Te ($x = 0.05$ and 0.10) for the first time by chemical co-precipitation method using thiophenol as a surfactant. Particle sizes in the range of $3 - 5$ *nm* were obtained with cubic zinc-blende phase. The samples showed photoluminescence in the red region with composition dependent emission wavelength. The intensity of emission decreases with increasing dopant concentration of Mn and Te. EPR analysis proves the presence of Mn as a substitutional dopant in place of Zn in the zinc blende structure of ZnS nanopartiles with paramagnetic nature at room temperature and also the EPR spectra supported the photoluminescence studies.

The authors are highly grateful to the University Grants Commission, New Delhi, Govt. of India, for providing the financial support. One of the authors, Ms. A. Divya, is thankful to C.S.I.R., New Delhi, for awarding Senior Research Fellowship.

REFERENCES

1. X.F. Duan, Y. Huang, Y. Cui, J. Wang, C.M. Lieber, *Nature* **409**, 66 (2001).
2. A.N. Shipway, E. Katz, I. Willner, *Chem. Phys. Chem.* **1**, 18 (2000).
3. A.A. Guzelian, U. Banin, A.V. Kadavanich, X. Peng, A.P. Alivisatos, *Appl. Phys. Lett.* **69**, 1432 (1996).
4. A.D. Yoffe, *Adv. Phys.* **42**, 173 (1993).
5. T. Toyama, D. Adachi, M. Fujii, Y. Nakano, H. Okamoto, *J. Non-Cryst. Solids* **299-302**, 1111 (2002).
6. M. Behboudnia, P. Sen, *Phys. Rev. B* **63**, 035316 (2001).
7. J. Huang, Y. Yang, S. Xue, B. Yang, S. Liu, J. Shen, *Appl. Phys. Lett.* **70**, 2335 (1997).
8. S.C. Qu, W.H. Zhou, F.Q. Liu, N.F. Chen, Z.G. Wang, H.Y. Pan, D.P. Yu, *Appl. Phys. Lett.* **80**, 3605 (2002).
9. A.A. Bol, R.V. Beek, A. Meijerink, *Chem. Mater.* **14**, 1121 (2002).
10. R.N. Bhargava, D. Gallagher, X. Hong, A. Nurmiko, *Phys. Rev. Lett.* **72**, 416 (1994).
11. D.D. Awschalom, J.M. Kikkawa, *Phys. Today* **52**, 33 (1999).

12. P.H. Borse, D. Srinivas, R.F. Shinde, S.K. Date, W. Vogel, S.K. Kulkarni, *Phys. Rev. B* **60**, 8659 (1999).
13. B.D. Cullity, S.R. Stock, *Elements of X-ray Diffraction*, 3rd Ed. (Prentice hall: 2001).
14. N.M. Rao, D.R. Reddy, B.K. Reddy, C.N. Xu, *Phys. Lett. A* **372**, 4122 (2008).
15. D. Son, D.R. Jung, J. Kim, T. Moon, C. Kim, B. Park, *Appl. Phys. Lett.* **90**, 101910 (2007).
16. H. Li, W.Y. Shih, W.H. Shih, *Nanotechnology* **18**, 205604 (2007).
17. C. Falcony, M. Garcia, A. Ortiz, J.C. Alonso, *J. Appl. Phys.* **72**, 1525 (1992).
18. W. Tang, D.C. Cameron, *Thin Solid Films* **280**, 221 (1996).
19. Z. Quan, Z. Wang, P. Yang, J. Lin, J. Fang, *Inorg. Chem.* **46**, 1354 (2007).
20. H. Nikol, A. Vogler, *Inorg. Chem.* **32**, 1072 (1993).
21. P. Benalloul, J. Benoit, A. Geoffrey, D. Yebdri. R. Bilewicz, W. Busse, H.E. Gumlich, R. Rebentisch, *J. Cryst. Growth* **101**, 976 (1990).
22. S.C. Erwin, L. Zu, M.I. Haftel, A.L. Efros, T.A. Kennedy, D.J. Norris, *Nature*, **436**, 91 (2005).
23. A. Abragam, B. Bleaney, *EPR Spectra of Transition Metal Ions*, (Oxford Press: 1970).
24. D. Bleanny, R.S.A. Rubbins, *Proc. Phys. Soc. Jpn*. **77**, 103 (1961).
25. N.M. Rao, R.P. Vijayalakshmi, D.R. Reddy, B.K. Reddy, *Spectrochimi. Acta Part A* **69**, 688 (2008).